

Modelling of Interbranch Coupled 1:2 Tree Microstrip Interconnect

B. Ravelo¹, A. Normand², and F. Vurpillot²

¹Normandy University, UNIROUEN, ESIGELEC, IRSEEM EA 4353
Technopole du Madrillet, Avenue Galilée, BP 10024, F-76801 Saint Etienne du Rouvray, France

²Normandy University UNIROUEN, GPM UMR 6643, F-76000 Rouen, France
ravelo@esigelec.fr

Abstract — A computational method of unbalanced single-input two-output (1:2) interconnect with coupled interbranch is introduced. The circuit theory is built with the topology constituted by the octopole Z-matrix represented by the coupled lines. The voltage transfer functions (VTFs) and the input impedance of the input-output electrical path of the unbalanced 1:2 tree with interbranch coupled lines are established. The computation model is verified with proofs of concept (POC) constituted by unbalanced 1:2 tree microstrip structure with and without interbranch coupled phenomenon. The POCs are loaded by resistors and capacitors. Good agreements between the simulated and modelled VTFs and the overall structure input impedances were obtained from 0.1-to-2 GHz.

Index Terms — Circuit theory, coupled lines, microstrip interconnect, modelling methodology, transmission line, tree network,

I. INTRODUCTION

With the increase of the integration density and design complexity, the printed circuit board (PCB) performance depends on the interconnect effects [1]. The PCB interconnects play important roles during the design and manufacturing. The PCB design technological roadblocks consist in the interconnect effects modelling. The high-density interconnects cause unintentionally the transmitted signal distortions, latency due to the degradation generated by unwanted perturbations. To predict these breakthroughs, intensive research works have been performed high speed PCB signal distribution interconnect computational methods [2-4]. The PCB interconnect design requires consistent transmission line (TL) model. It enables to predict the signal degradation and unintentional effects. The PCB interconnect computation becomes one of the most attractive research topics of electronic design and manufacturing [2-4]. Initially, the PCB, packaged and integrated circuits (ICs) interconnect network was modeled with first order approximation of the equivalent

transfer function by Elmore in 1948 [5]. The initial computational model is elaborated with RC-network. It presents advantages in terms of simplicity and its possibility for fast delay estimation of different paths of integrated system. However, the Elmore model accuracy is drastically decreasing when the signal speed is increased. Therefore, this computation method is limited to simple interconnect networks. Therefore, further improvement is required to increase the accuracy. In late 1970s, improved RC network model was introduced by Wyatt [6-7]. In 1980s, the improved model was widely used. Significant performance of the signal delay modelling for the typically linear RC-meshes of tree networks was performed [7-8]. In 1990s, the RC-model was extended to the prediction of the behaviors of more complex networks as dominant time constant MOS VLSI circuit design and manufacturing [9]. The employed computation algorithm for estimating the propagation delay times for multi-levels of tree mesh networks composed of cascaded RC-cells is to sum the delays at each node of the circuits. Nevertheless, the RC-tree network model is less efficient when the PCB operating signal speed is increased.

Recently, more accurate second order approximated RLC model taking into account the inductance effect with closed form of delay times (propagation, rise/fall and settling time delays) were developed [10-11]. The modelling method allowing to determine the unit step response of RLC tree networks from second moments of the polynomial transfer function was proposed [11]. More accurate tree model promising to approximate the over- or under-damped responses and the basic characteristics as the second order propagation delay expression were also deployed [11]. Moreover, modelling and simulation techniques of TL networks were suggested [12]. The second order model was also employed for estimating the delay associated to non-monotone time-domain responses of high speed tree interconnect networks [13-14]. The RLC-model was extended to the modelling of high performance interconnection structures as on-chip architecture buses,

multiphase multiplexer clock system [15] and arbitrary level high-speed digital-analog converters [16]. However, the accuracy of these models and the computation time needs to be improved when the tree distribution level is higher. To face out this limitation, more general behavioral model for extracting the analytical transfer function of multi-levels of signal distributed tree networks was developed in [17-19]. This PCB tree interconnect network model is fundamentally consisted of cascaded L-cells and distributed TLs. By using the transfer matrix theory, the whole network transfer function was expressed. However, the available model of PCB tree interconnects does not integrate the electromagnetic (EM) crosstalk and coupling problem between the interconnect line branches [20-21]. The crosstalk affects the system of serial links as in the mobile terminal emitter [21].

For this reason, the unbalanced tree interconnects modelling with interbranch EM coupling effect is developed in this paper. Section II describes the computational theory of interbranch coupled unbalanced single-input double-output (1:2) tree. Section III is the unbalanced 1:2 tree input impedance and the voltage transfer functions (VTFs) model validations with Advanced Design System (ADS®) simulations. Section IV is the conclusion.

II. INTERBRANCH COUPLED 1:2 TREE INTERCONNECTS MODEL

The proposed computational method is aimed to the determination of the input impedance and the unbalanced tree interconnect VTFs. In difference with the existing models, the proposed one integrates the coupling phenomenon interbranch of the unbalanced tree interconnects. In more concrete view, the tree under study is composed of elementary TLs configured as depicted in Fig. 1.

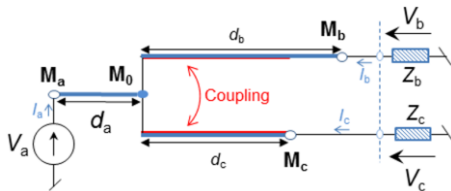


Fig. 1. Unbalanced tree interconnect structure.

The electrical network is constituted by three branches TL_{MaM0} , TL_{M0Mb} and TL_{M0Mc} . The characteristic impedances and physical lengths are respectively (Z_a, d_a) , (Z_b, d_b) and (Z_c, d_c) by supposing that $d_b > d_c$. Moreover, the output branches TL_{M0Mb} and TL_{M0Mc} are implicitly with EM coupling phenomenon.

A. Equivalent circuit topology

The posed problem can be traduced by the

unbalanced 1:2 tree interconnect modelling. It consists in the transformation of the initial tree network introduced in Fig. 1 into the systemic model depicted in Fig. 2. The voltages across the nodes M_a , M_b and M_c are respectively denoted $V_a = V_{Ma}$, $V_b = V_{Mb}$ and $V_c = V_{Mc}$.

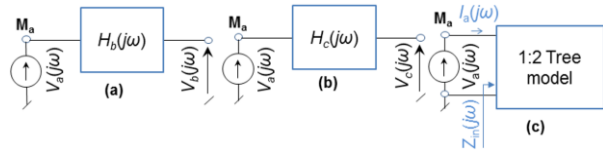


Fig. 2. VTF equivalent circuit systemic view: (a) H_a , (b) H_b , and (c) input impedance Z_{in} .

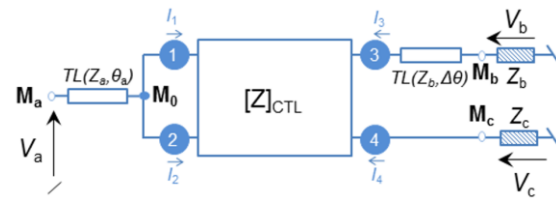


Fig. 3. Equivalent circuit diagram of the unbalanced tree interconnect including the CTL Z-matrix.

The system VTFs and overall input impedance are defined by:

$$H_b(j\omega) = V_{M_b}(j\omega) / V_{M_a}(j\omega) = V_b(j\omega) / V_a(j\omega), \quad (1)$$

$$H_c(j\omega) = V_{M_c}(j\omega) / V_{M_a}(j\omega) = V_c(j\omega) / V_a(j\omega), \quad (2)$$

$$Z_{in}(j\omega) = V_a(j\omega) / I_a(j\omega), \quad (3)$$

with ω is the angular frequency. The equivalent circuit diagram of the unbalanced 1:2 tree can be elaborated by considering the impedance- or Z-matrix of the coupled TL (CTL). The modelling method can be established from the equivalent circuit diagram presented in Fig. 3. The unbalanced tree structure can be transformed as an electrical network mainly constituted by elementary TLs. We assume that the input is connected the TL TL_{MaM0} characterized by $TL(Z_a(j\omega), \gamma_a(j\omega))$. TL_{M0Mb} and TL_{M0Mc} , respectively characterized by $TL(Z_b(j\omega), \gamma_b(j\omega))$ and $TL(Z_c(j\omega), \gamma_c(j\omega))$ constitute the output branches. With $\xi = \{a, b, c\}$, $Z_\xi(j\omega)$ is the characteristic impedance and $\gamma_\xi(j\omega) = \alpha_\xi(j\omega) + j\beta_\xi(j\omega)$ is the propagation constant (ω is the angular frequency, α_ξ is the attenuation constant, β_ξ phase constant associated to the electrical length $\theta_\xi = \beta_\xi d_\xi$). These output networks can be represented by the coupled TL matrix $[Z]_{CTL}$ and the output TL $TL(Z_b(j\omega), \Delta\gamma(j\omega))$ associated to the electrical length $\Delta\theta$. This CTL structure is assumed as an octopole with Ports ① and ② interconnected, and Ports ③ and ④ are connected to output loads R_b and R_c . Each access port m ($m = \{1, 2, 3, 4\}$) is traversed by branch currents I_m .

Let us denote C the coupling coefficient between the coupled lines connecting Ports ① and ②, and Ports

③ and ④ and $Z_0(j\omega)$ is the characteristic impedance of each elementary line. According to the TL theory, the even- and odd-characteristic impedances of the associated coupled lines constituting the unbalanced 1:2 tree is defined as $Z_e=Z_0[(1+C)/(1-C)]^{0.5}$ and $Z_o=Z_0[(1-C)/(1+C)]^{0.5}$. The lengths of the input and output TLs can be characterized by the resonance angular frequencies ω_ξ which are linked to the physical length by the relation $d_\xi=2\pi v/\omega_\xi$ with $\xi=\{a,b,c\}$ and the wave speed v . Moreover, the physical length difference $\Delta d=d_b-d_c$ between the $TL_{M_0M_b}$ and $TL_{M_0M_c}$ corresponding to the quarter wavelengths $\lambda_b/4$ and $\lambda_c/4$ is also equivalent to the electrical length analogue to the overlength TL connecting Port ③ and node M_b . The equivalent electrical length is associated to Δd . It is analytically equal to $\Delta\theta = \beta_b \Delta d = \beta_b (d_b - d_c)$. It implies the relation $\Delta\theta = \pi\omega(\omega_c - \omega_b)/(2\omega_b \cdot \omega_c)$. The associated input impedance, which is spontaneously related to the TL characteristic impedance $Z_0(j\omega)$, is given by $Z(j\omega) = Z_0(j\omega) / \tanh[\Delta\gamma(j\omega)]$.

B. Z-Matrix of the coupled output branches and access line ABCD or transfer matrices

The adopted methodology to solve the posed-problem is fundamentally based on the calculation of the branch currents. The Z-matrix of the tree coupled branches and the access line ABCD matrices must be expressed in function of the interconnect structure parameters. The four-port CTL structure constituting the unbalanced 1:2 tree can be represented by the equivalent 4×4 Z-matrix analytically expressed as:

$$[Z] = \begin{bmatrix} Z_{11} & Z_{12} & Z_{13} & Z_{14} \\ Z_{21} & Z_{22} & Z_{23} & Z_{24} \\ Z_{31} & Z_{32} & Z_{33} & Z_{34} \\ Z_{41} & Z_{42} & Z_{43} & Z_{44} \end{bmatrix}. \quad (4)$$

By denoting α the attenuation constant and d the physical length, based on the microwave theory and due to the symmetry, the matrix elements are defined as:

$$\begin{cases} Z_{11} = Z_{22} = Z_{33} = Z_{44} = \frac{Z_e + Z_o}{2 \tanh(\alpha d + j\theta)} \\ Z_{12} = Z_{21} = Z_{34} = Z_{43} = \frac{Z_e - Z_o}{2 \tanh(\alpha d + j\theta)}, \\ Z_{13} = Z_{31} = Z_{24} = Z_{42} = \frac{Z_e - Z_o}{2 \sinh(\alpha d + j\theta)} \\ Z_{14} = Z_{41} = Z_{23} = Z_{32} = \frac{Z_e + Z_o}{2 \sinh(\alpha d + j\theta)} \end{cases}, \quad (5)$$

with $\theta = \pi\omega/(2\omega_c)$. Furthermore, the ABCD matrices

analytically equivalent to the TL connecting the node M_a -Port ①, and Port ③-node M_b are respectively defined as [17-18]:

$$[T_a] = \begin{bmatrix} A_a & B_a \\ C_a & D_a \end{bmatrix} = \begin{bmatrix} \cosh(\gamma_a) & Z_a \sinh(\gamma_a) \\ \sinh(\gamma_a)/Z_a & \cosh(\gamma_a) \end{bmatrix}, \quad (6)$$

$$[T_b] = \begin{bmatrix} A_b & B_b \\ C_b & D_b \end{bmatrix} = \begin{bmatrix} \cosh(\Delta\gamma) & Z_{b_0} \sinh(\Delta\gamma) \\ \sinh(\Delta\gamma)/Z_{b_0} & \cosh(\Delta\gamma) \end{bmatrix}. \quad (7)$$

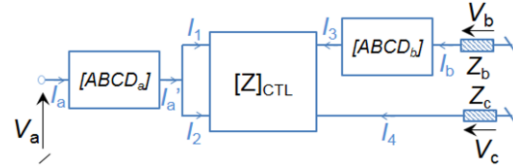


Fig. 4. Reduced two-port equivalent network of the circuit introduced in Fig. 2.

The abstracted topology equivalent to the unbalanced 1:2 tree structure under study can be represented as highlighted in Fig. 4. This topology enables to realize the theorization of the problem with the analogue mathematical concept. The branch currents $[I_1, I_2, I_3, I_4, I_a, I_b]$ are assumed as the unknown variables which must be expressed in function of the input excitation source V_a . Meanwhile, the problem solution can be reformulated as the calculation of the tree branch currents $I_a, I_a', I_1, I_2, I_3, I_4$ and I_b . The algebraic solution can be determined from linear equations derived via the combination of the impedance- and ABCD-matrices in (4), (6) and (7), and the Ohm's laws applied to the output loads Z_b and Z_c :

$$V_b = -Z_b \cdot I_b, \quad (8)$$

$$V_c = -Z_c \cdot I_c. \quad (9)$$

Moreover, at the junction node M_0 , we have the relation $I_a' = I_1 + I_2$ and $V_1 = V_2$. By taking this condition into account, the following synthetic equation system can be deduced from the access line ABCD matrices associated to (8) and (9):

$$\begin{cases} V_a = A_a V_1 + B_a (I_1 + I_2) \\ I_a = C_a V_1 + D_a (I_1 + I_2) \\ V_3 = A_b V_b - B_b I_b = -(A_b Z_b + B_b) I_b \\ I_3 = C_b V_b - D_b I_b = -(C_b Z_b + D_b) I_b \end{cases}. \quad (10)$$

The voltage and current vectors $[V] = [V_1 V_2 V_3 V_4]$ and $[I] = [I_1 I_2 I_3 I_4]$ corresponding to the configuration of the coupled lines presented in the circuit diagram of Fig. 3 are linked to the Z-matrix defined in (4) by the equation system:

$$[V] = [Z]_{CPTL} [I] \Leftrightarrow \begin{cases} V_1 = Z_{11}I_1 + Z_{12}I_2 + Z_{13}I_3 + Z_{14}I_4 \\ V_2 = Z_{21}I_1 + Z_{22}I_2 + Z_{23}I_3 + Z_{24}I_4 \\ V_3 = Z_{31}I_1 + Z_{32}I_2 + Z_{33}I_3 + Z_{34}I_4 \\ V_4 = Z_{41}I_1 + Z_{42}I_2 + Z_{43}I_3 + Z_{44}I_4 \end{cases} \quad (11)$$

C. VTF and input impedances of the tree input-output electrical path

The combination of (10) and (11) implies the following synthetic characteristic equation system of the posed-problem mathematical solution knowing the excitation source V_a in (12). The main access branch currents I_a and I_b can be yielded from the solutions via the ABCD matrices of TLMs TLM_{MaM0} and $TLM_{Port0-Mb}$ in (13). Consequently, the unbalanced 1:2 tree characteristic matrix derived from (12) and (13) can be written in (14):

$$\begin{cases} (Z_{11} + \frac{B_a}{A_a})I_1 + (Z_{12} + \frac{B_a}{A_a})I_2 + Z_{13}I_3 + Z_{14}I_4 = \frac{V_a}{A_a} \\ (Z_{21} + \frac{B_a}{A_a})I_1 + (Z_{22} + \frac{B_a}{A_a})I_2 + Z_{23}I_3 + Z_{24}I_4 = \frac{V_a}{A_a} \\ Z_{31}I_1 + Z_{32}I_2 + (Z_{33} - \frac{A_b Z_b + B_b}{C_b Z_b + D_b})I_3 + Z_{34}I_4 = 0 \\ Z_{41}I_1 + Z_{42}I_2 + Z_{43}I_3 + (Z_{44} + Z_c)I_4 = 0 \end{cases} \quad (12)$$

$$\begin{cases} I_a = [C_a V_a + (D_a A_a - B_a)(I_1 + I_2)] / A_a \\ I_b = -I_3 / (C_b Z_b + D_b) \end{cases} \quad (13)$$

$$\begin{bmatrix} \frac{V_a}{A_a} \\ \frac{V_a}{A_a} \\ 0 \\ 0 \\ \frac{C_a V_a}{A_a} \\ 0 \end{bmatrix} = \begin{bmatrix} Z_{11} + \frac{B_a}{A_a} & Z_{12} + \frac{B_a}{A_a} & Z_{13} & Z_{14} & 0 & 0 \\ Z_{21} + \frac{B_a}{A_a} & Z_{22} + \frac{B_a}{A_a} & Z_{23} & Z_{24} & 0 & 0 \\ Z_{31} & Z_{32} & Z_{33} - \frac{A_b Z_b + B_b}{C_b Z_b + D_b} & Z_{34} & 0 & 0 \\ Z_{41} & Z_{42} & Z_{43} & Z_{44} + Z_c & 0 & 0 \\ \frac{B_a}{A_a} - D_a & \frac{B_a}{A_a} - D_a & 0 & 0 & 1 & 0 \\ 0 & 0 & 1 & 0 & 0 & C_b Z_b + D_b \end{bmatrix} \begin{bmatrix} I_1 \\ I_2 \\ I_3 \\ I_4 \\ I_a \\ I_b \end{bmatrix} \quad (14)$$

By taking $x = \tanh(\alpha d + j\theta)$, the VTF through the 1:2 tree electrical path $M_a M_b$ can be expressed as:

$$H_b(j\omega) = \frac{Z_b(j\omega)I_b(j\omega)}{-V_a(j\omega)} = \frac{\sqrt{1-x^2}}{\chi_2^b x^2 + \chi_1^b x + \chi_0^b}, \quad (15)$$

where

$$\begin{cases} \chi_2^b = 2Z_o \begin{bmatrix} B_a((B_b + A_a Z_b) - (D_b + C_b Z_b)Z_c) \\ -A_a(D_b + C_b Z_b)Z_e^2 \end{bmatrix} \\ \chi_1^b = \begin{bmatrix} A_a(A_a Z_b + B_b - (D_b + C_b Z_b)Z_c)Z_e^2 \\ +4B_a(B_b + A_a Z_b)Z_c \\ + \begin{bmatrix} A_a(4A_a Z_b + B_b) - (4B_a(D_b + C_b Z_b)) \\ +A_a D_b Z_c + A_a C_b Z_b Z_c \end{bmatrix} Z_o Z_e \end{bmatrix} \\ \chi_0^b = 2Z_e B_a \begin{bmatrix} B_a(B_b + A_a Z_b) + Z_c(A_a B_b - B_a D_b) \\ +(A_a^2 - B_a C_b)Z_b \end{bmatrix} \end{cases} \quad (16)$$

Similarly, the VTF equivalent to the electrical path $M_a M_c$ can be written as:

$$H_c(j\omega) = \frac{Z_c(j\omega)I_4(j\omega)}{-V_a(j\omega)} = \frac{Z_b + D_b + B_b + A_a Z_b}{\chi_2^b x^2 + \chi_1^b x + \chi_0^b} [Z_o x (C_b \sqrt{1-x^2})] \quad (17)$$

The overall structure input impedance can be extracted from (3).

III. VALIDATION RESULTS

This section is focused on the validations of the developed unbalanced 1:2 model. Two POC of unbalanced 1:2 trees are designed by considering the aspects with and without interbranch coupled branches. The POC modelled computed results are compared with simulations run in the ADS® environment of the electronic circuit designer and simulator. AC simulations are considered by assigning the voltage excitation source V_a with 201 frequency samples from 0.1 GHz to 2 GHz.

A. Description of the POC

The POC represented in 3D view in Figs. 5 are microstrip passive distributed circuits which are interconnect passive structures of unbalanced 1:2 tree networks. The arbitrarily chosen structures with and without output interbranch coupling are respectively shown in Fig. 5 (a) and Fig. 5 (b).

These microstrip structures were printed on the dielectric substrate Kapton® polyimide film provided by DuPont® with characteristics relative permittivity $\epsilon_r=3.3$, loss tangent $\tan(\delta)=0.008$, thickness $h=125 \mu\text{m}$, conductivity $\sigma=58 \text{ MS/m}$ and thickness $t=17 \mu\text{m}$. Both sides of the film were laminated with copper layer, forming the ground plane for the unbalanced 1:2 tree interconnects circuit, and the layer on which the circuit was patterned respectively. Knowing the POC characteristics, the demonstrator circuit was designed with elementary lines presenting arbitrary physical

parameters. The POCs with and without interbranch coupling presents physical sizes are respectively $28\text{ mm}\times 75\text{ mm}$ and $122\text{ mm}\times 29\text{ mm}$. The POC structures are excited by the AC voltage source V_a and loaded by Z_b and Z_c connected at the output nodes M_b and M_c . Acting as an AC or frequency analysis, the input voltage source was fixed equal to constant $V_a=1\text{ V}$ for the discrete frequency f varied from 0.1-to-2 GHz with 201 frequency samples.

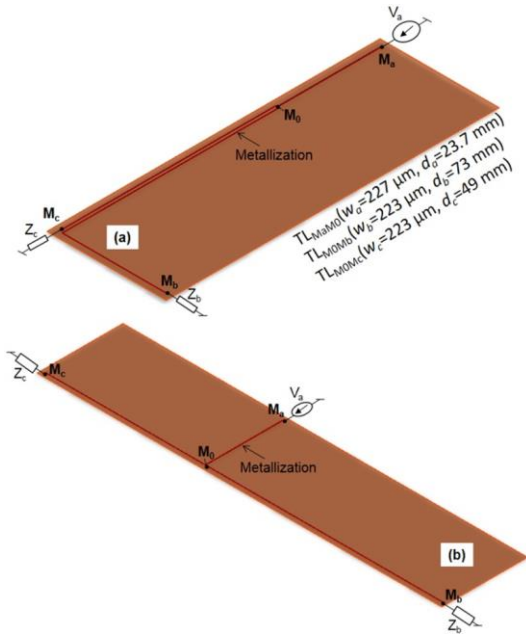


Fig. 5. 3D design of the POC asymmetrical 1:2-tree microstrip structure: (a) with and (b) without output interbranch coupling.

B. POC circuit physical, electrical and EM characteristics

The POC were designed with arbitrary parameters which prove the influence of the interbranch coupling on the two VTFs. The microstrip line effective permittivity and characteristic impedances were extracted based on the microstrip TL theory. The coupled branch parameters ($C=-10\text{ dB}$, $Z_c=69.37\ \Omega$, $Z_o=36.04\ \Omega$, $s=40\ \mu\text{m}$) were extracted. The modelling and simulations were performed with these different parameters. However, the entire proposed model computed results were realized with Matlab programming. During the calculations, the ideal parameters were supposed independent to the frequency and the TL losses were neglected. The equivalent model was developed by assuming the $TL_{MaMo}(w_a=227\ \mu\text{m}$, $d_a=23.7\text{ mm}$, $Z_a=50\ \Omega$) with the frequency quarter wavelength $f_a=2\text{ GHz}$ and the coupled lines $TL_{MOMb}(w_b=223\ \mu\text{m}$, $d_b=73\text{ mm}$, $Z_b=56.5\ \Omega$) and $TL_{MOMc}(w_c=223\ \mu\text{m}$, $d_c=49\text{ mm}$, $Z_c=56.5\ \Omega$) are defined with the frequency quarter wavelengths $f_b=1\text{ GHz}$ and $\Delta f=2\text{ GHz}$. The minimal

physical width of the microstrip structure which can be fabricated with the equipment available in our laboratory is limited to $300\ \mu\text{m}$. For this reason, the POC fabricated prototypes are not available for the present study. The branch currents were computed.

C. Applications with resistive loaded unbalanced tree

In this case, the impedance loads are assigned as lumped resistors with nominal values $Z_b=50\ \Omega$ and $Z_c=100\ \Omega$. The VTF magnitudes $|H_a|$ and $|H_b|$ are respectively displayed in Fig. 6 (a) and Fig. 6 (b). These results illustrate the relevance and effective of the developed model for the interbranch coupling phenomenon prediction. Without coupling, more accentuated resonance effects are observed at the terminal M_a and M_b . The interbranch coupling effects can be predicted by the proposed computation method in good agreement with the simulations from very low frequencies to 2 GHz. The same remark is found with the input impedance magnitude $|Z_{in}|$ of the overall structure plotted in Fig. 7. The VTF model accuracy presents error absolute maximal value of about 1 dB. The highest absolute differences between the simulations and modelled results are reasonably appeared around the resonance frequencies. The main difference between the model and the reference simulations are caused by the characteristics of the elementary TLs constituting the unbalanced tree structure. Furthermore, these discrepancies increase at higher frequencies. Such effects are mainly due to the influence of the frequency on the TL EM and electrical parameters as the skin depth effect and the substrate dispersion.

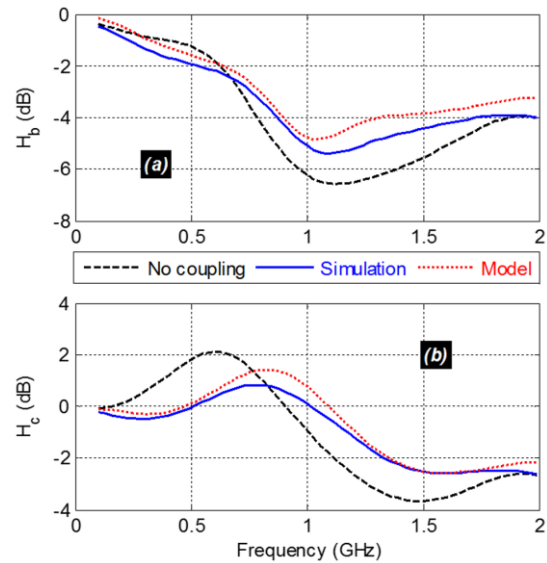


Fig. 6. Comparison of modelled and simulated resistive loaded tree interconnect VTF magnitudes: (a) $|H_b|$ and (b) $|H_c|$.

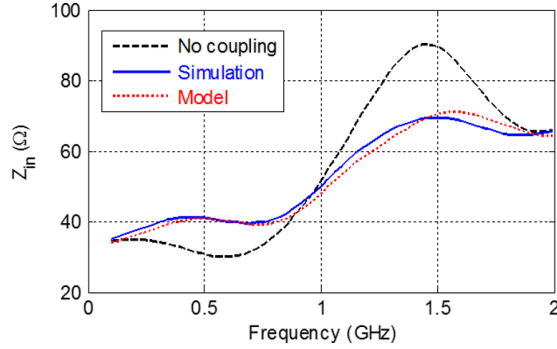


Fig. 7. Comparison of the modelled and simulated resistive loaded tree interconnect input impedance magnitude $|Z_{in}|$.

These computation errors are also added to the numerical computation inaccuracies.

To generate the modelled computed results with the assigned samples, the computation speed was less than one millisecond by using a PC equipped a single-core processor Intel® Core™ i3-3120M CPU @ 2.50 GHz and 8 GB physical RAM with 64-bits Windows 7.

D. Applications with capacitive loaded unbalanced tree

In this case, the impedance loads are constituted by arbitrary chosen lumped resistor $Z_b=50 \Omega$ and capacitor $Z_c=1 \text{ pF}$. The frequency simulations were carried out with the unbalanced 1:2 tree structure by sweeping the AC source V_a frequency. Then, comparison between the simulations and computed models is realized. The obtained VTF magnitudes $|H_a|$ and $|H_b|$ are respectively displayed in Fig. 8 (a) and Fig. 8 (b). Once again, without coupling, the resonance effects are occurred slightly at lower frequencies. The simulated and modelled VTFs are in good agreement for the different types of output loads Z_b and Z_c . A notable well-correlated behavior of the VTFs versus frequency is observed with simulations and the developed modelling methods in the considered broadband frequency band. The comparison between the associated input impedances magnitude $|Z_{in}|$ can be seen in Fig. 9. Similar to the previous case, the interbranch coupling influences obviously, the unbalanced tree frequency responses notably when the frequency is higher than 0.5 GHz. Despite the coherent behavior between the modeled and simulated results, numerical discrepancies appear around the resonance frequency situated between 0.5 GHz and 1 GHz.

This noteworthy deviation is mainly due to the approximation of the TL electrical and EM characteristics which are assumed to be independent to the frequency during the computation process.

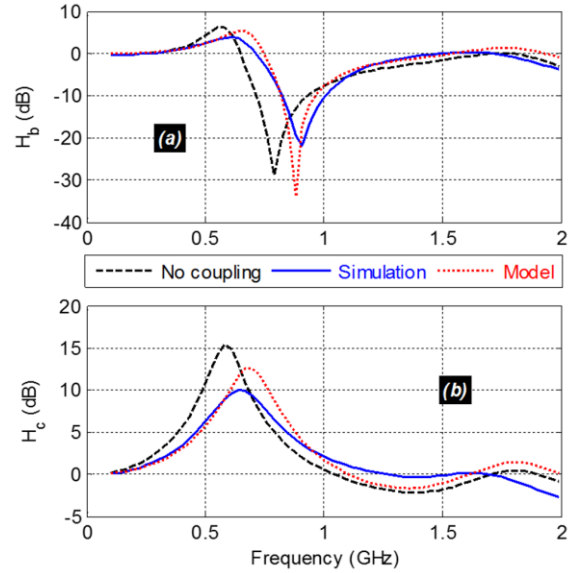


Fig. 8. Comparison of the modelled and simulated capacitive loaded tree interconnect VTF magnitudes: (a) $|H_b|$ and (b) $|H_c|$.

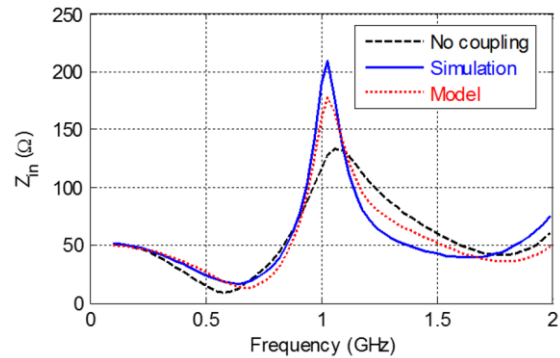


Fig. 9. Comparison of the modelled and simulated capacitive loaded tree interconnect input impedance magnitude $|Z_{in}|$.

IV. CONCLUSION

A circuit theory on 1:2 tree interconnects with interbranch coupling is established. The model is built with the combination of the coupled lines octopole impedance matrix and the access line ABCD matrices. The equivalent topology enables to traduce the system into the problem mathematical abstraction. The VTF of the tree input-output electrical path and the overall circuit input impedance are established. Two POCs constituted by unbalanced 1:2 tree with and without interbranch coupling are designed. The modeled and simulated tree input-output VTFs and also the input impedance are compared via AC simulations from 0.1- to-2 GHz. Good agreements between simulations and

the models are observed. The proposed computation method is more efficient in terms of precision with the EM coupling influence compared to the methods available in [17-19] which are dedicated to the linear tree VTF modelling.

ACKNOWLEDGMENT

Acknowledgement is made to the Normandy Region for the BRIDGE project support of this research work through the FEDER fund.

REFERENCES

- [1] C. Schuster and W. Fichtner, "Parasitic modes on printed circuit boards and their effects on EMC and signal integrity," *IEEE Trans. EMC*, vol. 43, no. 4, pp. 416-425, Nov. 2001.
- [2] H. Husby, "High Density Interconnect," White Paper, Data Response. Available Online [2016]. <http://www.datarespons.com/high-density-interconnect/>
- [3] B. Archambeault and A. E. Ruehli, "Analysis of power/ground-plane EMI decoupling performance using the partial-element equivalent circuit technique," *IEEE Trans. EMC*, vol. 43, no. 4, pp. 437-445, Nov. 2001.
- [4] K. M. C. Branch, J. Morsey, A. C. Cangellaris and A. E. Ruehli, "Physically consistent transmission line models for high-speed interconnects in lossy dielectrics," *IEEE Trans. Advanced Packaging*, vol. 25, no. 2, pp. 129-35, Aug. 2002.
- [5] W. C. Elmore, "The transient response of damped linear networks," *J. Appl. Phys.*, vol. 19, pp. 55-63, Jan. 1948.
- [6] L. Wyatt, *Circuit Analysis, Simulation and Design*. North-Holland. The Netherlands: Elsevier Science, 1978.
- [7] D. Standley and J. L. Wyatt, Jr., "Improved Signal Delay Bounds for RC Tree Networks," VLSI Memo, No. 86-317, MIT, Cambridge, MAS (USA), May 1986.
- [8] J. Rubinstein, P. Penfield, Jr., and M. A. Horowitz, "Signal delay in RC tree networks," *IEEE Trans. CAD*, vol. 2, no. 3, pp. 202-211, July 1983.
- [9] L. Vandenberghe, S. Boyd, and A. El Gamal, "Optimizing dominant time constant in RC circuits," *IEEE Trans CAD*, vol. 17, no. 2, pp. 110-125, Feb. 1998.
- [10] A. B. Kahng and S. Muddu, "An analytical delay model of RLC interconnects," *IEEE Trans. CAD*, vol. 16, pp. 1507-1514, Dec. 1997.
- [11] A. Ligocka and W. Bandurski, "Effect of inductance on interconnect propagation delay in VLSI circuits," *Proc. of 8th Workshop on SPI*, Heidelberg, Germany, pp. 121-124, 9-12 May 2004.
- [12] A. Deutsch, et al., "High-speed signal propagation on lossy transmission lines," *IBM J. Res. Develop.*, vol. 34, no. 4, pp. 601-615, July 1990.
- [13] J. Cong, L. He, C. K. Koh, and P. H. Madden, "Performance optimization of VLSI interconnect layout," *Integration VLSI J.*, vol. 21, no. 1-2, pp. 1-94, Nov. 1996.
- [14] L. Xiao-Chun, M. Jun-Fa, and T. Min, "High-speed clock tree simulation method based on moment matching," *Proc. of Prog. In Electromagnetics Research Symposium (PIERS) 2005*, Hangzhou, China, vol. 1, no. 2, pp. 142-146, 22-26 Aug. 2005.
- [15] L. Hungwen, S. Chauchin, and L. J. Chien-Nan, "A tree-topology multiplexer for multiphase clock system," *IEEE Trans. CAS I: Regular Papers*, vol. 56, no. 1, pp. 124-131, Feb. 2009.
- [16] N. Rakuljic and I. Galton, "Tree-structured DEM DACs with arbitrary numbers of levels," *IEEE Trans. CAS I: Regular Papers*, vol. 52, no. 2, pp. 313-322, Feb. 2010.
- [17] B. Ravelo, "Behavioral model of symmetrical multi-level T-tree interconnects," *Prog. In Electromagnetics Research B*, vol. 41, pp. 23-50, 2012.
- [18] B. Ravelo, "Modelling of asymmetrical interconnect T-tree laminated on flexible substrate," *Eur. Phys. J. Appl. Phys.*, vol. 72, no. 2 (20103), pp. 1-9, Nov. 2015.
- [19] B. Ravelo and O. Maurice, "Kron-Branin modelling of Y-Y-tree interconnects for the PCB signal integrity analysis," *IEEE Trans. EMC*, vol. 59, no. 2, pp. 411-419, Apr. 2017.
- [20] D. S. Gao, A. T. Yang, and S. M. Kang, "Modeling and simulation of interconnection delays and crosstalks in high-speed integrated circuits," *IEEE Trans. CAS I*, vol. 37, no. 1, pp. 1-9, Jan. 1990.
- [21] M. Voutilainen, M. Rouvala, P. Kotiranta, and T. Rauner, "Multi-gigabit serial link emissions and mobile terminal antenna interference," *Proc of 13th IEEE Workshop on SPI*, Strasbourg, France, pp. 1-4, May 2009.

B. Ravelo holds his Ph.D. degree in 2008 from Univ. Brest and his HDR in 2012 from Univ. Rouen. He is currently Associate Professor at ESIGELEC/IRSEEM in Rouen (France). His research interests cover the microwave circuit design, EMC, and signal/power integrity (SI/PI) engineering. He is a pioneer of the negative group delay (NGD) concept for RF/analog and digital circuits and systems. He is (co)-author of more than 200 national/international papers. His current publication h-index is 15 (Reference: Google Scholar 2017).

A. Normand is born in Normandy (France), where he is confronted with his first experiment in scientific instrumentation. He joined the laboratory GPM UMR 6634 where he had the opportunity to develop several technical aspects of the tomographic atom probe (SAT). In 2005, he has worked for few months in the Laboratory of Materials Analysis in Göttingen (Germany) to develop a 3D field ion microscope. After receiving

master's degree in Scientific Instrumentation from the Univ. Rouen in 2007, he integrated, as an Instrumental Design Engineer, the ERIS Research Team to develop the SAT and its correlative techniques.

F. Vurpillot is currently a Professor at GPM UMR 6634, Univ. Rouen. His research interest is on the SAT scientific instrumentation.